CHAPTER 27

On Wave Deformation After Breaking

Toru Sawaragi
Professor of Civil Engineering
Osaka University, Osaka, Japan

and

Koichiro Iwata
Lecturer of Civil Engineering
Osaka University, Osaka, Japan

ABSTRACT

Waves will dissipate their energy rapidly after breaking. In this paper, the three factors , (i) formation of a horizontal roller, (ii) bottom friction, and (iii) turbulence with air entrainment, which will contribute to the energy dissipation, are dealt with experimentally and theoretically

The horizontal roller formed by a plunging breaker is approximated as a Rankine-type vortex by experiments, and it is calculated that 15%-30% of wave energy is dissipated due to the formation of horizontal roller alone from a breaking point to a point of the roller disappearance.

A bottom shear stress due to a breaker is measured by the shear meter deviced by the authors and it is clarified that the energy dissipation due to bottom friction is a little

Main part of the energy dissipation is taken to be caused by the turbulence with air entrainment. It is indicated that an incident monocromatic wave is transformed into a higher frequency wave due to the turbulence. Furthermore, a new basic equation for breaking waves with a turbulence term expressed by a Reynolds stress is presented The theoretical curves computed numerically have a consistent agreement with the experimental results

1 INTRODUCTION

Phenomenon of wave breaking and wave deformation after breaking has been a matter of great interest to coastal engineers as well as investigations in the hydrodynamic field. Therefore, so far, in the experimental and theoretical approaches, numerous investigations have been done to clarify the mechanism of wave deformation in a surf zone

In the theoretical treatments, many investigations have assumed model waves such as solitary wave and bore with some appropriate assumptions that waves have their critical heights as progressive waves, etc However, these theoretical works could not explain sufficiently the mechanism of wave deformation after breaking. In the experimental investigations various studies have been carried out mainly on a sloping beach model. There necessarily exist, in the sloping beach model, return flow, wave set-up and set-down, wave shoaling and wave reflection Since these factors interact very complicatedly, the important characteristics of turbulence caused by wave breaking, can not be clarified in details. Mason(1951) already pointed out the necessity of experimental investigations on a horizontal bottom Galvin (1969) carried out some experiments on a composite slope consisted of an approach ramp with a 1/15 slope leading up to a horizontal surface and showed facts about the characteristics at the breaking point. But the mechanism of wave deformation after breaking was not discussed

As above mentioned, these foregoing investigations seem to be unable to clarify the mechanism of wave deformation or wave energy dissipation in a surf zone Thus, the application of a more special experimental method to reveal the characteristics of turbulence itself or a more reasonable theoretical treatment will be required

The present paper is to clarify the mechanism of wave deformation and energy dissipation in experimental and theoretical treatments

2 BEHAVIOR OF WAVES AFTER BREAKING

2-1 Equipment and Procedure

Experiments were conducted to clarify such hydrodynamic behaviors of waves at a breaking point and after breaking as breaker types, scale of splash and horizontal roller, wave height attenuation, etc., by using an indoor wave tank in 0.7m width, 0 95m height and 30m length At one end of the tank was installed a flap-type wave generator which was controlled by an electric dynamic shaker and could generate waves in different periods and amplitudes At the other end of the tank, a horizontal bottom was installed and connected to the channel bottom with a slope of 1/18 as shown in Fig -1 In this horizontal bottom, there are no return flow and shoaling effect as observed in a sloping beach Therefore, turbulence itself caused by breaking can be deduced Wave heights were measured by resistance-type wave gauges A wave height in deep water, H_o, is calculated by the small-amplitude wave theory (Wiegel,1964) from a measured wave height in front of the wave generator For each experimental run, by using a high speed cine-camera(100-200 frames/sec), the breaking region was filmed through a grid on glass walls of the channel with the camera axis kept at the still water level From these films, the scale of the horizontal roller, the domain of the roller existence, the scale of splash and the region of air entrainment in the breaker were decided. To obtain the movement of water particles in the breaker, particles of a mixture of xylen and carbontetrachloride with zinc oxide for coloring, with a specific gravity corresponding to that of the water, were introduced in the surf zone Point to point movement of the particles was then recorded on films, from which each particle velocity was obtained by superposition of projected film frames to give a distance and a time interval of movement Wave heights in the breaking zone was estimated as ten-wave averages from wave gauge recorders compareing with film analyses The incident waves were forced to break themselves on a horizontal bottom or just at the corner between the elevated horizontal bed and the sloping bed The test program is shown in Table-1.

h	Ho	To	Ho/Lo
7 cm	3 5 ~ 11 5 cm	0 8, 1 0, 1 2 sec	0 016 ~ 0 115
11 cm	6 0 ~ 12 0 cm	0 8, 1 0, 1 2 sec	0 031 ~ 0 105
14 cm	7 5 ~ 13 5 cm	0 8, 1 0, 1 2 sec	0 033 ~ 0 105

Table - 1. Test program

2-2 Experimental Results

Breaker type and breaker height

A breaker is classified into a plunging breaker and a spilling breaker as shown in Fig -2 But a surging breaker (or a collapsing breaker) occurring in a sloping beach is not observed in this case Therefore, the surging breaker is a particular breaking pattern in a sloping beach The transient region between the two breaker types is given as follows

$$H_o / h_b = 0\ 72 \qquad (1)$$

Fig -3 shows the relation between wave steepness, H_o/L_o, and the ratio, H_b/h_b of breaker height H_b and water depth h_b It is recognized that H_b/h_b becomes larger as H_o/L_o is larger and that H_b/h_b for a plunging breaker is larger than that for a spilling breaker

Characteristics of turbulence after breaking

The pattern of wave deformation after breaking is clearly different between a plunging breaker and a spilling breaker In case of the plunging breaker, as shown in Fig -4(a), there exist a horizontal roller and a splash The horizontal roller draws air bubble deep into the water body and the air bubble rises rapidly upwards as the roller disappears On the other hand, in case of the spilling breaker, as shown in Fig -4(b), keeping the symmetry of wave forms at the crest, a white cap is observed at the cusped-crest and the air entrainment is limitted on the wave front face In Fig -4, the origin of X is just a breaking point and X_B, X_V, X_S and X_A indicate a point where a wave crest touches down the water, a roller disappears, a splash touches down the water and air bubble disappears from the water body, respectively Fig -5 shows the relation of X_B/L, X_V/L, X_S/L, X_A/L and H_o/L_o, where L is the wave length at the depth of h calculated by the small-amplitude wave theory(Wiegel,1964) It is recognized that the relation of $X_B/L \leqq X_V/L \leqq X_S/L \leqq X_A/L$ is established and that X_A/L is largely affected by h/L_o and H_o/L_o Judging from Fig -3, X_A/L for a

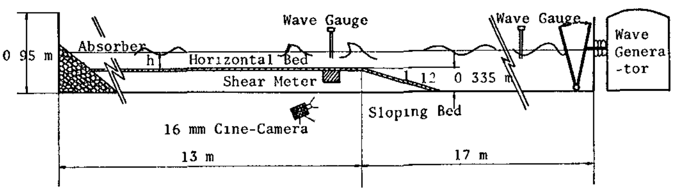

Fig.- 1 Laboratory installation

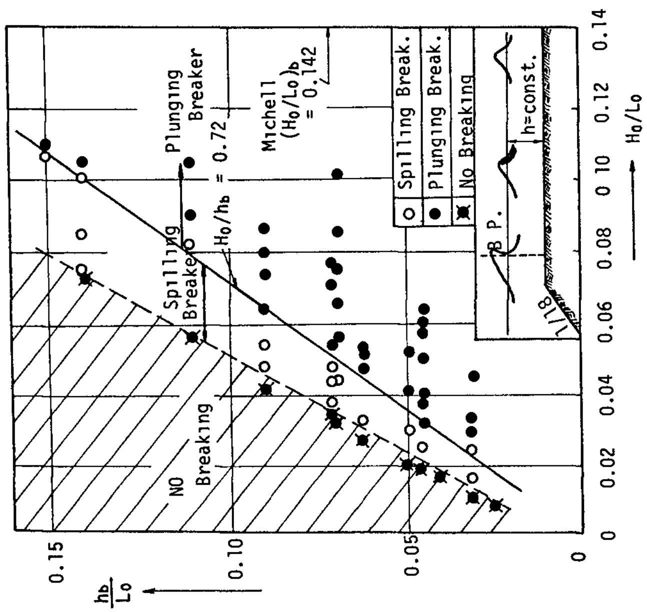

Fig.-2. Breaking pattern and breaking criteria.

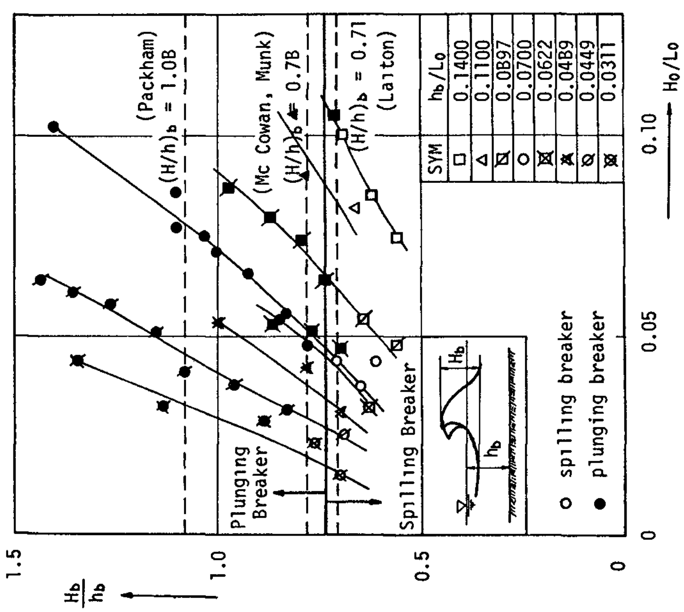

Fig.- 3. Breaker height .

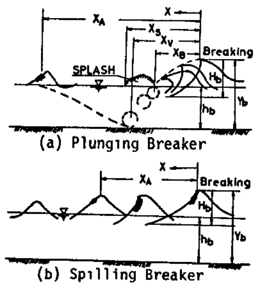

Fig.-4 Sketch of charateristics of wave breaking pattern.

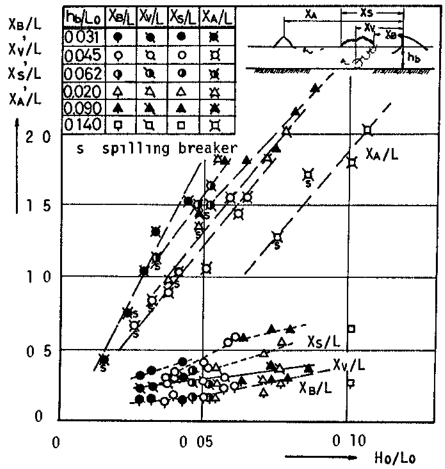

Fig -5 Relation among X_B/L, X_V/L, X_S/L, X_A/L and H_0/L_0

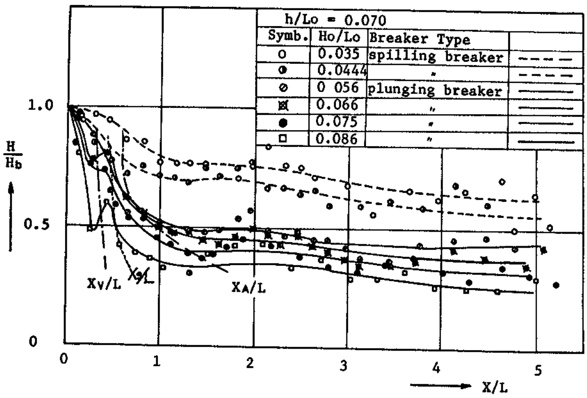

Fig.-6. Wave height attenuations after breaking (h/L_0=0 070) plunging breaker is recognized to be larger than that for a spilling breaker Fig -6 shows a wave height attenuation after breaking. It is made clear that the degree of wave height attenuation becomes larger as H_o/L_o is larger and that it is closely connected to the turbulence of breaking waves That is, the wave height attenuation for $X/L \leq X_A/L$ is larger than that for $X/L \geq X_A/L$ In case of a plunging breaker, the wave height attenuation is the largest for $X/L \leq X_V/L$, which indicates that some of the energy is transmitted into the kinematic energy of the horizontal roller

3 EFFECT OF HORIZONTAL ROLLER ON WAVE ENERGY DISSIPATION

The hydrodynamic characteristics of the roller were made clear by the above-mentioned experiments in Section 2 As shown in Fig -7, the distribution of the angular velocity of the roller is approximated as a Rankine type vortex so that the angular velocity can take a maximum value at $r = r_o$ In the experiments, r_o is nearly equal to 0 $44H_b$ as shown in Fig -8

Now, consider the effect of the horizontal roller on wave energy dissipation The kinematic energy, E_r, of this roller is defined as follows (Hino,1971)

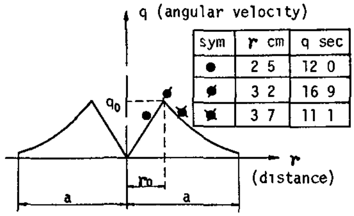

Fig -7 Distribution of an angular velocity of horizontal roller

$$E_r = \frac{1}{4}\rho\pi(q_o r_o)^2(1 + 4\ln(a/r_o)) \quad \text{---------(2)}$$

where q_o=angular velocity at $a=r_o$, ρ= water density

If the breaking wave energy is assumed to be expressed as the same expression as before breaking, the energy dissipation from the breaking point to the point of the roller disappearance, E_L,is given as follows

$$E_L = \frac{1}{8}\rho g(H_b^2 - H_v^2)L \quad \text{---------(3)}$$

where H_v=wave height at a point of the roller disappearance Therefore, the rate of energy transmitted to this roller, ε_r, is given in Eq (4)

$$\varepsilon_r = \frac{E_r}{E_L} = \frac{2\pi(q_o r_o)^2(1 + 4\ln(a/r_o))}{gL(H_b^2 - H_v^2)} \quad \text{---------(4)}$$

Now, putting the relation of r_o=0 $44H_b$ into Eq (4), the following expression is obtained

$$\varepsilon_r = \frac{1\ 216 q_o^2(1 + 4\ln(a/r_o))}{gL(1 - (H_v/H_b)^2)} \quad \text{--------(5)}$$

Fig -9 shows the theoretical values of Eq (5) and the experimental results The theoretical values show that ε_r takes a larger value as q_o^2/qL becomes larger and a/r_o becomes larger The experimental results indicate that 15%-30% of the energy dissipation of wave is transmitted into the kinematic energy of the roller. Therefore, it is concluded that the most of the energy will be dissiapted by the other factors such as bottom friction, splash and turbulence with air entrainment, etc

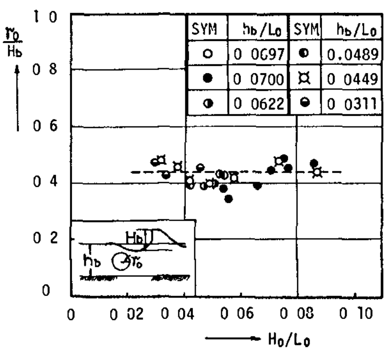

Fig -8 Relation between r_o/H_b and H_o/L_o.

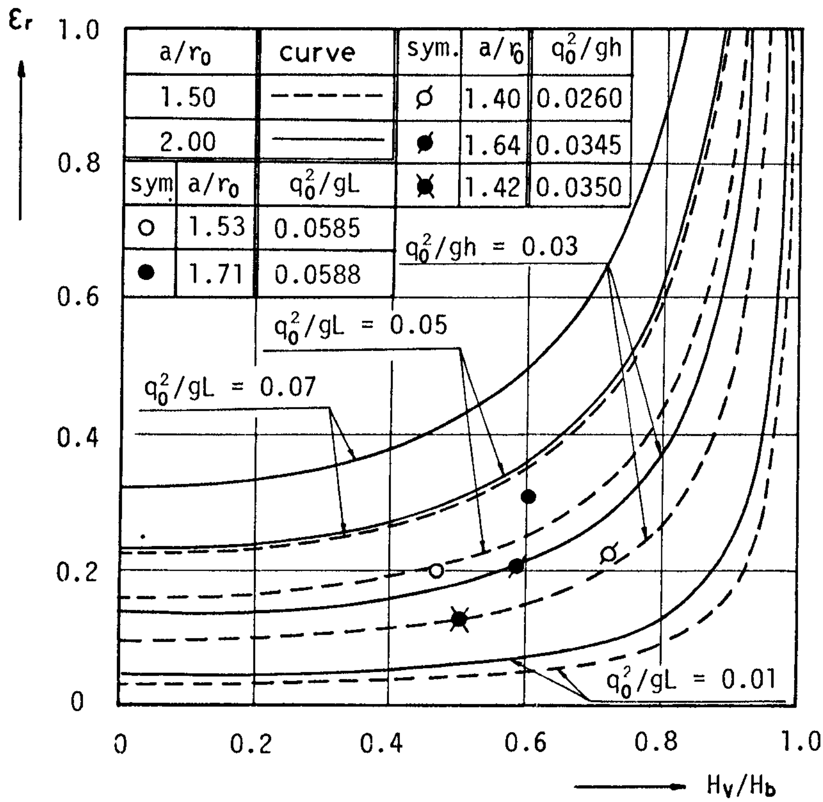

Fig.-9. Relation between $\mathcal{E}_r$ and H_V/H_b.

4 EFFECT OF BOTTOM FRICTION ON WAVE ENERGY DISSIPATION

4-1 Equipment and Procedure

A bottom shear stress due to wave motion was measured by the shear meter deviced by the authors A schematic view of the shear meter is shown in Fig -10 A small raised channel was set transversely from wall to wall of the frame below the shear plate To prevent flow through gaps under the plate, the channel was filled with mercurry until its meniscus touched the underside of the shear plate as Eagleson (1962) already deviced If the flow under the shear plate is not stopped, the pressure gradient is different between above and below the shear plate, which causes a force acting in the opposite direction to the original wave force

A shear force acting on the shear plate is measured by converting the force into a moment of the supporting shaft The shear plate is subjected to a force due to wave pressure gradient in addition to the shear force Therefore, the force due to the pressure gradient is calculated from the pressure difference measuered by pressure measuring tubes Before measuring bottom friction force due to breaking waves, the shear meter was checked under various laminar conditions, and it is recognized that the results coincide well with the theoretical values as shown in Table-2, in which theoretical values are calculated by using the theory of Iwagaki-Tuchiya-Chin (1965)

4-2 Experimental Results

Fig -11 shows time profiles of a bottom shear stress and a wave , and it indicates that the time prifiles of the shear stress due to a plunging breaker is very asymmetric as compared with those in the case of a spilling breaker Fig.-12 shows change of non-dimensional maximum bottom shear stresses which act in the wave propagation direction and its opposite direction for the two type of breakers In Fig - 12, X is a distance from a breaking point and the dotted lines express the shear stress estimaeted by the smooth laminar boundary layer theory(Iwagaki- Tuchiya-Chin,1965)given as follows

$$\frac{\tau_{b\,max}}{\rho g H} = \frac{\sqrt{2\nu}}{g \sinh(kh)}\left(\frac{\pi}{T}\right)^{3/2} , \qquad (5)$$

where, ν = kinematic fluid viscosity, $\tau_{b\,max}$ = maximum bottom shear stress, $k=2\pi/L$, ρ = fluid density and H=wave height at the depth of h

From this figure, it will be pointed out that the maximum bottom shear stresses in the region for $X \leqq X_A$ are considerably larger than those in the region for $X > X_A$ Therefore,it is made clear that the bottom shear stresses become larger due to the turbulence with air entrainment As shown in Fi -11, the time profiles of the bottom shear stresses are very asymmetric, and then the coefficient of the bottom friction used earlier can not be applied Then, the newly defined bottom friction coefficient, $\hat{C}_f$, is used in this study, which is defined as follows

$$\hat{C}_f = \frac{1}{2\pi}(\theta_c \hat{C}_{fc} + \theta_t \hat{C}_{ft}) , \qquad (6)$$

$$\left.\begin{aligned} \hat{C}_{fc} = 2\left|\overline{\tau}_{bc}\right| / \left|\overline{U}^2_{bc}\right| \quad , \quad \hat{C}_{ft} = 2\left|\overline{\tau}_{bt}\right| / \left|\overline{U}^2_{bt}\right| \\ \theta_c + \theta_t = 2\pi \end{aligned}\right\} , \qquad (7)$$

where θ = phase, U_{bc} = horizontal bottom particle velocity moving toward wave propagation direction, U_{bt} = horizontal bottom particle velocity moving toward anti-wave propagation direction, τ_{bc} = bottom shear stress acting toward wave propagation direction, τ_{bt} = bottom shear stress acting anti-wave propagation direction, and the sign, — indicates mean value about the time

Fig -13 indicates the change of $\hat{C}_f$ as waves propagate, from which $\hat{C}_f$ is recognized to have no clear characteristics as waves propagate Fig -14 shows the relation among $\hat{C}_f$, $\hat{C}_{ft}$, $\hat{C}_{fc}$ and Reynolds number R_θ (= $\hat{U}_b^2 \cdot T/\nu$) It is shown that $\hat{C}_f$, $\hat{C}_{ft}$, $\hat{C}_{fc}$ become larger as R_θ is smaller But, the experimental values are generally larger than the theoretical value, $\hat{C}_f$= 4 5 $R_\theta^{-1/2}$ based on the smooth laminar boundary layer theory(Iwagaki-Tuchiya-Chin,1965)

The coefficient of bottom friction, f , already used in the fields observations is defined as follows(Putnam-Johnson,1949).

$$f = \tau_{b\,max} / \rho u_{b\,max}^2 \quad , \qquad (8)$$

where $\tau_{b\,max}$ = maximum bottom shear stress, $U_{b\,max}$ = maximum horizontal particle velocity at the bottom

Fig -15 shows the relation between f and Reynolds number R_{eT}(= $U_{b\,max}^2 \cdot T/\nu$), in which the straight line indicates the theoretical values based on the smooth laminar boundary layer theory The experimental values after breaking indicate 2 - 4 times larger than the theoretical value, $f = 2\ 08 R_{eT}^{-1/2}$ (Iwagaki-kakinuma-miyai,1965)

Now, the energy dissipation due to bottom friction is discussed The mean energy loss, $\bar{E}_{fb}$, due to the bottom friction per unit area is calculated by the following equation

$$\bar{E}_{fb} = \frac{1}{T}\int_0^T \bar{U}_b \bar{\tau}_b \, dt \quad , \qquad (9)$$

where $\bar{U}_b$ and $\bar{\tau}_b$ are a mean value of horizontal particle velocity and a shear stress at the bottom in the region of the same sign under wave motion, respectively On the other hand, the following relation is derived by the energy balance for a wave

$$\frac{d}{dx}(C_g E) = \bar{E}_{fb} + \bar{E}_{ft} \quad , \qquad (10)$$

where C_g = group velocity of wave, E = wave energy , and $\bar{E}_{ft}$ = mean energy loss due to some other causes than the bottom friction

If E and C_g satisfy Eq (11),the ratio, ε , of energy loss due to the bottom friction to the total energy loss for dx is represented by Eq.(12) as follows·

$$\left.\begin{aligned} E &= \frac{1}{8}\rho g H^2 \\ C_g &= C \end{aligned}\right\} \quad , \qquad (11)$$

$$\varepsilon = \frac{\bar{E}_{fb}}{\frac{d}{dx}(C_g E)} = \frac{4\int_0^T \bar{\tau}_b \cdot \bar{U}_b \, dt}{gH \cdot T\ C\ (dH/dx)} \quad . \qquad (12)$$

Using the experimental values for wave height attenuation and shear stresses , ε is calculated by Eq (12) as shown in Table-3 From this calculation, it is clear that the energy loss due to the bottom friction is quite small, that is , while a wave propagate to the distance about the twice wave length, the rate of the energy loss due to the bottom friction takes 9% of the total energy at most

After all, it is concluded that the energy dissipation due to a horizontal roller and bottom friction is a little. Therefore, the authors have to admit that the turbulence with air entrainment is the most important factor for a wave decay after breaking

h (cm)	28	(water temperature = 8°c)						
T (sec)	0 8		1 0			1 2		
h/Lo	0 28		0 179			0 124		
H (cm)	0 4	1 25	1 0	1 16	1 56	0 66	1 19	1 57
(F_b max)ex (gr)	0 260	0 920	0 690	0 868	1 130	0 521	1 137	1 389
(τ_b max)ex (gr/cm²)	0 164	0 572	0 454	0 570	0 743	0 354	0 723	0 944
(τ_b max)theo.(gr/cm²)	0 176	0 500	0 500	0 520	0 780	0 376	0 678	0 895
(τ_b max)ex / (τ_b max)theo.	0.942	1 140	0.910	0.982	0 953	0 942	1 070	1 050

Table -2. Comparison of measured shear stresss with theoretical values under laminar boundary condition (ex =experiment,and theo =theory)

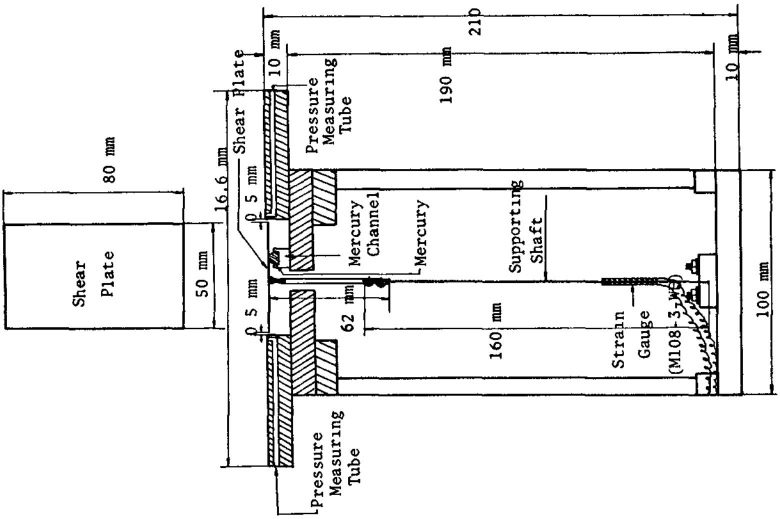

Fig.-10. Schematic view of the shear meter.

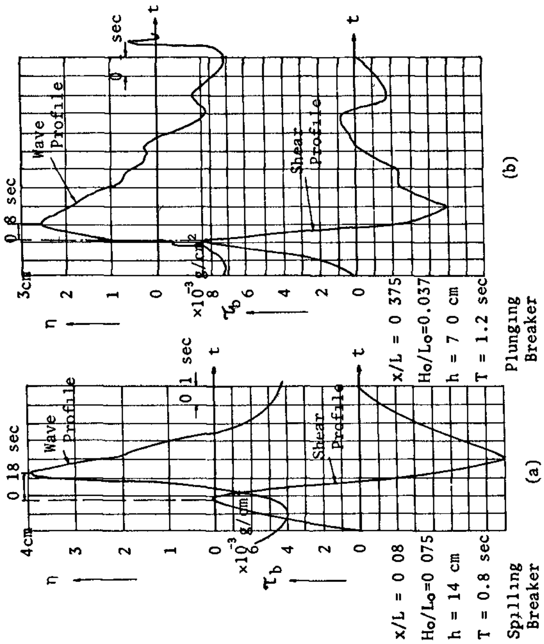

Fig.-11. Time-histories of shear stresses and waves.

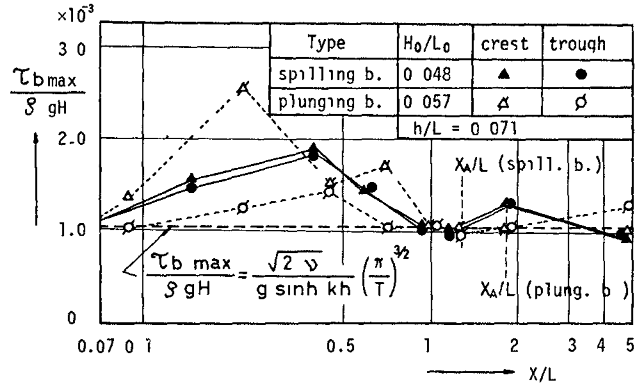

Fig.-12. An example of relations between $\tau_{b\,max}/\rho gH$ and X/L

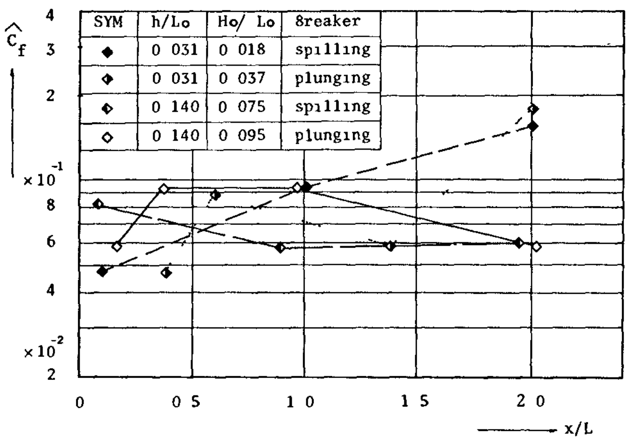

Fig.-13. Change of the coefficient, $\hat{C}_f$ as wave propagates

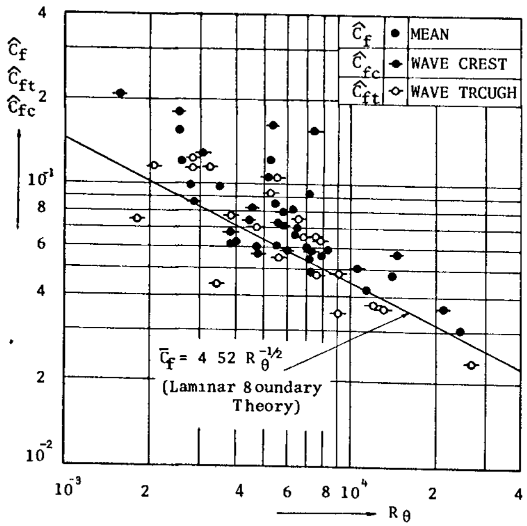

Fig -14. Relation among $\hat{C}_f, \hat{C}_{ft}, \hat{C}_{fc}$ and R_θ .

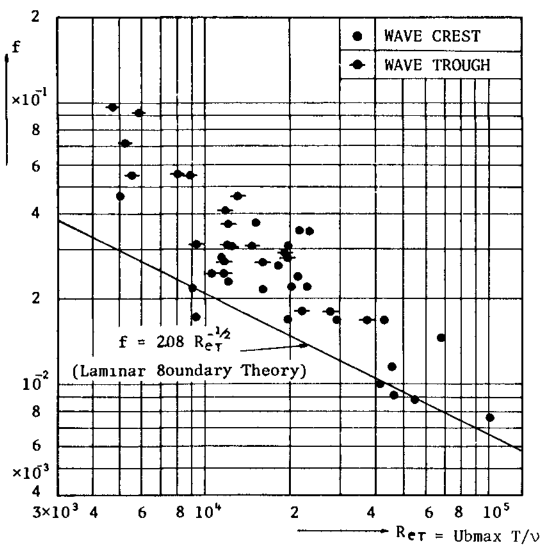

Fig.-15. Relation between f and R_{eT}.

RUN	h cm	T sec	H_b cm	H cm	x/L	$C/\sqrt{gh}$	$\epsilon\times10^2$	Breaker
5	7	1 2	5 0	4 4	0 25	1 07	0 8	spilling
"	"	"	"	2 7	1 40	0 97	4 0	"
"	"	"	"	2 6	2 10	0 94	8 9	"
6	7	1 2	8 0	5 0	0 30	1 07	0 6	plunging
"	"	"	"	3 2	1 50	1 14	4.2	"
"	"	"	"	2 7	2 20	1 03	5 5	"
13	14	0 8	6 3	5 4	0 85	0 87	1 7	spilling
"	"	"	"	4.9	1 30	0 99	2 2	"
"	"	"	"	4 6	2 00	0 94	7 7	"
14	14	0 8	9 5	5 4	0 95	0 94	1 0	plunging
"	"	"	"	5.0	1 30	0 99	1.9	"
"	"	"	"	4 7	2.05	0.94	2 6	"

Table -3 Calculated results of ϵ

5. EFFECT OF TURBULENCE ON WAVE ENERGY DISSIPATION

5-1 Fourier Analysis of Wave Profile

It is necessary to measure an accurate time-history of water particle velocity in order to clarify the characteristics of turbulence. It will be impossible on account of a lack of precise measuring instruments Since a wave profile is thought to be as an expression of turbulence after breaking, it will be expected that some features of turbulence can be deduced by analysing wave profiles The authors adopt Fourier analysis as one method, which can deduce characteristcs of frequencies of a wave.

Wave profiles were recorded by a magnetic-tape with sample time was 16 sec , and data were cut discretely at each 1/30 sec interval. The Fourier analysis was carried out by FFT method (Cooley-Tukey, 1965)

Figs.-16 - 18 show changes of wave height spectra as waves propagate At the breaking point, the wave is composed of harmonic frequencies against the monocromatic frequency of incident waves and immediately after breaking wave heights of the harmonic frequency waves become larger than those of the monocromatic incident waves As shown in Fig -19, however, the higher frequency waves disappear in a short time as the wave propagate after breaking. In the case of h/L=0.0311, as shown in Fig -17 and-18, the incident waves are transformed into higher frequency waves, such as twice or three times frequency waves of the incident waves, regardless of breaker types in the distance of three times the wave length from the breaking point. But, in the case of h/L_o=0 140(see Fig -16), the above-mentioned fact can not be observed. This means that the relative water depth, h/L_o plays an important role to transform a wave into a higer frequency wave rather than the breaking pattern , although this mechanism is not yet clear

5-2. Basic Equation for Breaking Wave

The mechanism of transformation of the monocromatic incident waves into higher frequency waves is very complicatedly Therefore, the authors avoid a direct discussion of this mechanism and only discuss a wave height attenuation by using the following turbulence model,

Two-dimensional Navier-Stokes equation with terbulence terms is given as follows(Ishihara-Homma, 1957)

$$\left.\begin{aligned} \rho\frac{DU}{Dt} &= -\frac{\partial P}{\partial x} + \mu\nabla^2 U + \left(\frac{\partial P_{xx}}{\partial x} + \frac{\partial P_{zx}}{\partial z}\right) \\ \rho\frac{DV}{Dt} &= -g - \frac{\partial P}{\partial z} + \mu\nabla^2 V + \left(\frac{\partial P_{zx}}{\partial x} + \frac{\partial P_{zz}}{\partial z}\right) \end{aligned}\right\} \quad (13)$$

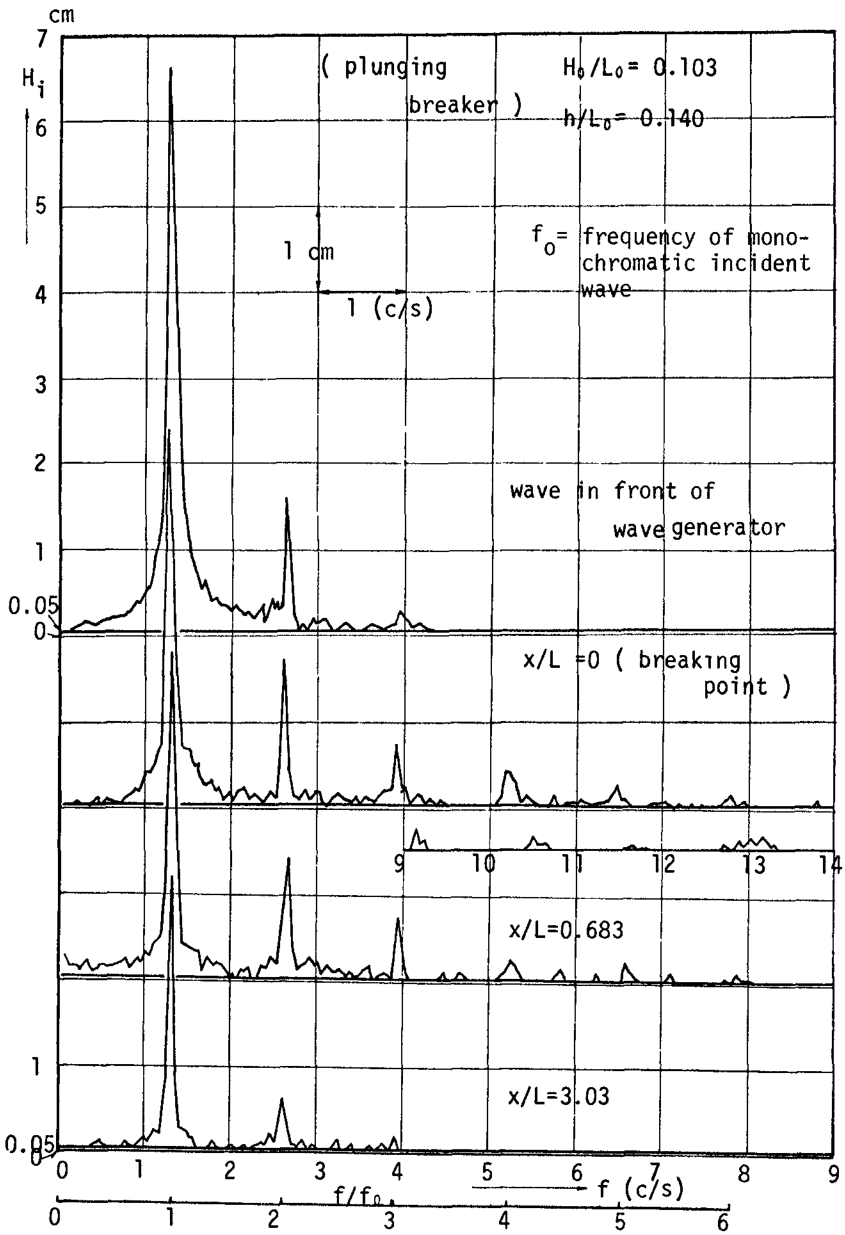

Fig.-16. Change of wave height spectrum. (h/L_0=0.140)

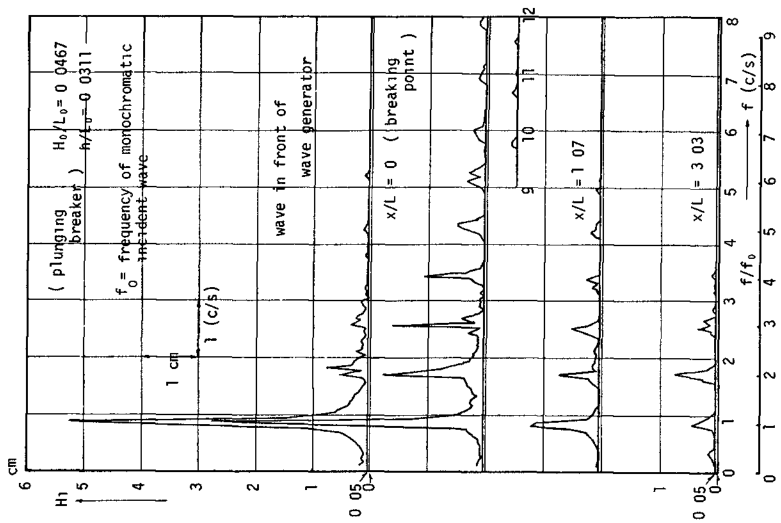

Fig -17 Change of wave height spectrum (h/L_0=0 0311)

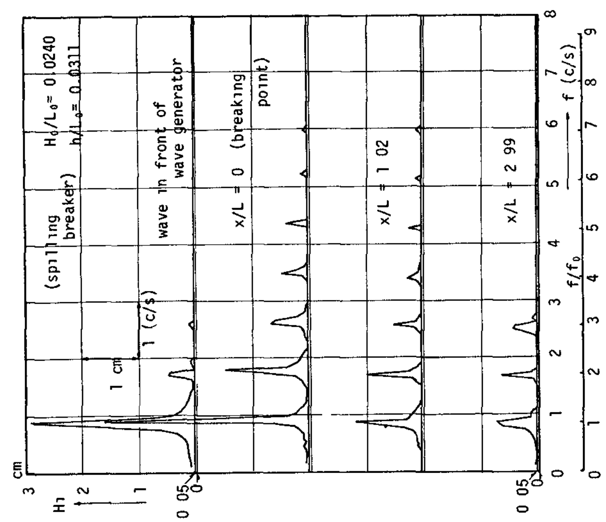

Fig -18 Change of wave height spectrum (h/L_0=0 0331)

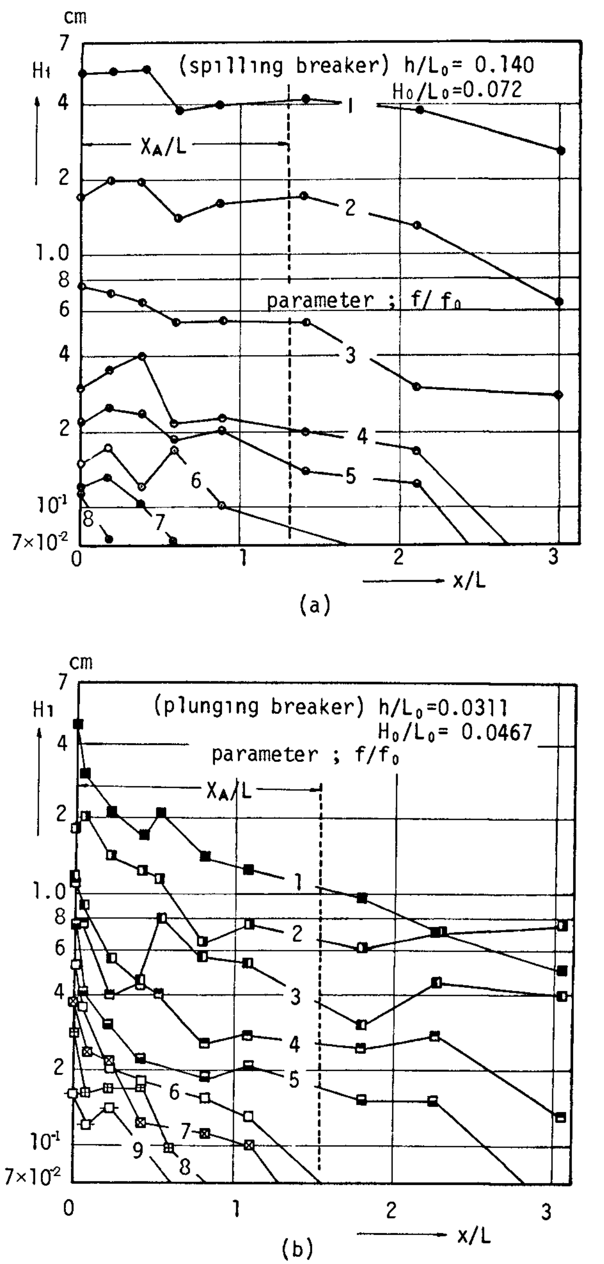

Fig.-19. Attenuation of wave heights of harmonic frequency waves as waves propagate.

where, P_{xx}, P_{zx} and P_{zz} = Reynolds stresses, $\nabla^2 = \frac{\partial^2}{\partial x^2} + \frac{\partial^2}{\partial z^2}$, μ = coefficient of fluid viscosity, g= gravity acceleration, t=time coordinate, p=pressure, V=vertical velocity of a water particle, U= horizontal velocity of a water particle, x = horizontal coordinate and z= vertical coordinate with the origin at the bottom

On the assumptions that (i) DV/Dt=0,(ii) terms due to molecular viscosity are considerably small as compared with terms due to Reynolds stress,(iii) ($O(\partial P_{xx}/\partial x)$ and $O(\partial P_{zx}/\partial x)$) $\gg$ ($O(\partial P_{zz}/\partial z)$ and $O(\partial P_{zx}/\partial z)$),Eq (13) is transformed into the following equation

$$\frac{\partial U}{\partial t} + U\frac{\partial U}{\partial x} + g\frac{\partial \eta}{\partial x} - \frac{\partial}{\partial x}(P_{xx} + P_{zx}) = 0 , \quad (14)$$

where η = wave profile

Assuming that P_{xx} and P_{zx} are able to be represented by the equation(15), the equation(14) is transformed into Eq.(16) as follows

$$\left.\begin{aligned} P_{xx}' &= L_1^2(\frac{\partial U}{\partial x})\left|\frac{\partial U}{\partial x}\right| \propto -L_x^2(\frac{U}{h})^2 \\ P_{zx} &= L_2^2(\frac{\partial U}{\partial z})\left|\frac{\partial U}{\partial z}\right| \propto -L_z^2(\frac{U}{h})^2 \end{aligned}\right\} \quad (15)$$

and

$$\frac{\partial U}{\partial t} + U\frac{\partial U}{\partial x} + g\frac{\partial \eta}{\partial x} + \frac{\partial}{\partial x}(K(\eta + h)^2(\frac{U}{h})^2) = 0 , \quad (16)$$

in which L_x and L_z = mixing length and $L_x^2 + L_z^2 = K (h + \eta)^2$ is assumed , where K is defined as the coefficient of turbulence intensity.

Therefore, the basic equations for a breaking wave are given as follows

$$\frac{\partial U}{\partial t} + U\frac{\partial U}{\partial x} + g\frac{\partial \eta}{\partial x} + \frac{\partial}{\partial x}(K (h + \eta)^2(\frac{U}{h})^2) = 0$$

and from the law of mass conservation (17)

$$\frac{\partial \eta}{\partial t} + \frac{\partial}{\partial x}(U (h + \eta)) = 0 .$$

Now. change the variables as follows

$$X^* = x/h , \quad T^* = (t/h)\sqrt{gh} , \quad U^* = U/\sqrt{gh} \quad \text{and} \quad H^* = (h + \eta)/ h , \quad (18)$$

then, Eq.(19) is obtained from Eq (17) by means of the finite difference method(Keller-Levine-Whitham, 1960) as follows

$$H^*(P) = \frac{1}{2}(H^*(R_1) + H^*(Q_1)) - \frac{\Delta T^*}{2\Delta X^*}(U^*(R_1)H^*(R_1) - U^*(Q_1)H^*(Q_1))$$

$$U^*(P) = \frac{1}{2}(U^*(R_1) + U^*(Q_1)) - \frac{\Delta T^*}{2\Delta X^*}(\frac{1}{2}(U^{*2}(R_1) - U^{*2}(Q_1)) + (H^*(R_1) - H^*(Q_1))) - K\frac{\Delta T^*}{2\Delta X^*}(H^{*2}(R_1)U^{*2}(R_1) - H^{*2}(Q_1)U^{*2}(Q_1)) \quad (19)$$

The numerical procedure is , in outline, to compute a wave height and velocity on a set of net points (X_i^*, T_k^*). In the calculation, the spatial net and time net are chosen to be uniform, $X_i^*=i\Delta X^*$ and $T_k^*=k\Delta T^*$, where, ΔT^* and ΔX^* are chosen to satisfy a stability condition, the so-called Courant Condition, stated as follows

$$\Delta T^* \leq \min_{P_i} \left(\frac{\Delta X^*}{U^*(P_i) + \sqrt{H^*(P_i)}} \right) . \quad (20)$$

The calculation is carried out by using the mesh width of ΔX^*=0 02 and ΔT^*=0.004, for which it was confirmed that the solutions were convergent and stable Unknown values, $H^*(P)$ and $U^*(P)$ at a point P, are calculated from the known values at point Q_1 and R_1 as shown in Fig.-20 by using Eq (19)

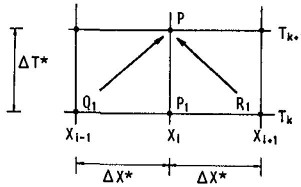

Fig -20 Mesh points

Fig.-21 shows the calculated values for wave height attenuation, in which the theoretical value of Horikawa-Kuo(1966) based on the energy method is also shown In this calculation, a solitary wave (Boussinesq,1872) is used as an intial wave condition From this figure, it is recognized that the degree of wave height attenuation becomes larger as K becomes larger and that the theoretical value for K=0 5 fairy agrees with the value of Horikawa-Kuo for β=5 Furthermore, Fig -22 shows that the theoretical values calculated by using experimental data as initial wave conditions considerably coincides with experimental results and that K for a plunging breaker is very large as compared with that for a spilling breaker

This fact indicates that the stronger the intensity of the turbulence, the greater the wave height attenuation, and therefore, it will be pointed out that the intensity of turbulence of the plunging breaker is larger than that for a spilling breaker

6 CONCLUSION

In this paper, wave deformation after breaking is discussed The energy dissipation after breaking is dominated by turbulence with air entrainment in the case of a spilling breaker In the case of a plunging breaker, some of the wave energy are dissipated by the formation of horizontal roller in addition to the turbulence with air entrainment Due to this turbulence, a monocromatic incident wave is transformed into a higher frequency wave in some condition This mechanism is unknown and it is required to clarify the characteristics of turbulence after breaking by a future investigation

REFERENCES

Mason,M A Some Observations of Breaking Wave, Gravity Waves,N B S Circular,521,1951.

Galvin, C J Breaker Travel and Choice of Design Wave Height, Proc. of ASCE, WW2,May, 1969

Wiegel, R L Oceanographical Engineering, Prentice-Hall, Englewood,Cliff,N J.,pp 11-21,1964

Hino,M and T Yamazaki, Formation of Roller and Energy Dissipation at Vertical Plate due to Wave, Proc of 18th Conf on Coastal Eng. in Japan, 1971 (in Japanese)

Eagleson,P S Laminar Damping of Oscillatory Waves, Proc of ASCE, Vol 88, No HY3 , 1962

Iwagaki,Y ,Y Tuchiya and K Chin Experimantal Study on Wave Attenuation due to Bottom Friction (3), Proc of 12 th Conf on Coastal Eng in Japan, 1965 (in Japanese)

Putnam,J A and J W Johnson The Dissipation of Wave Energy by Bottom Friction, Tran A G U , Vol.30, No 1,Feb ,1949.

Iwagaki,Y ,T. Kakinuma and H Miyai· On Bottom Friction Coefficient in Coastal Beaches, Proc. of 12th Conf on Coastal Eng in Japan, 1965 (in Japanese)

Cooley,J W. and J W Tukey An algorithm for the machine calculation of complex Fourier series, Math , Compt.,19, pp 297-301,1965

Ishihara,T and H.Homma Applied Hydraulics, Vol.1, Maruzen-Press, Tokyo, pp 35-40, 1957 (in Japanese)

Keller,H B ,D A Levine and G B Whitham Motion of a Bore over a Sloping Beach,Jour. of Fluid Mech , Vol.7, 1960

Boussinesq, J Théorie des ondes et des remous qui se propagent le long d'un canal rectangulaire horizontal, en communiquant au liquide contenu dans ce canal de vitesses sensiblement pareilles de la surface au fond, Liouville's J Math Vol.17, 1872

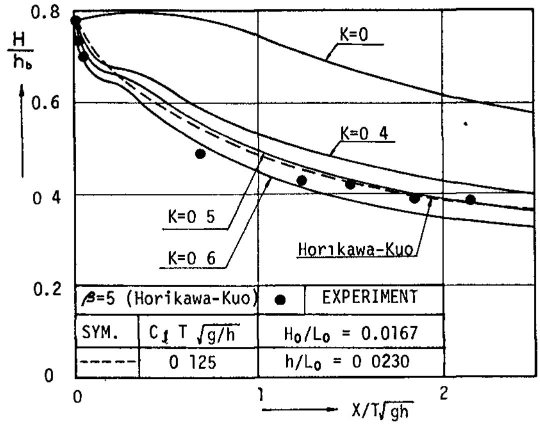

Fig -21. Theoretical values of wave height attenuations.(By using solitary wave as an initial wave condition)

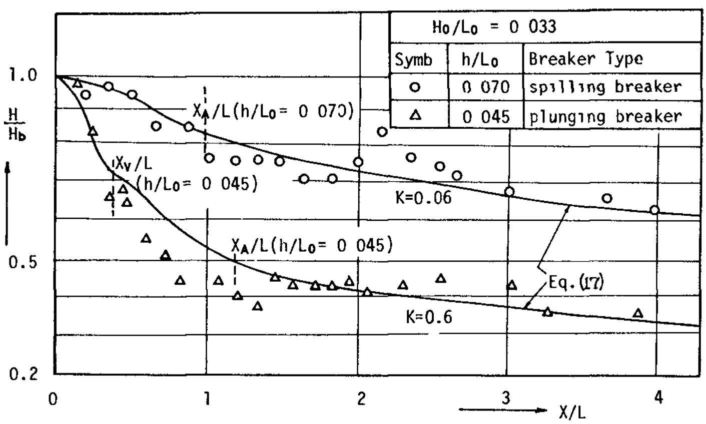

Fig.-22. Comparison of calculated theoretical values with experimental results. (By using experimental data as an initial wave condition)